Complex Systems 1 (1987) 633–647

Numerical Experiments on Lattice Gases: Mixtures and Galilean Invariance

Dominique d'Humières
Pierre Lallemand
Laboratoire de Physique de l'Ecole Normale Supérieure,
24 rue Lhomond, 75231 Paris Cedex 05, France

Geoffrey Searby
Laboratoire de recherche sur la combustion,
Centre de St Jérôme, 13397 Marseille Cedex 13, France

Abstract. In this paper, we first describe an extension of the standard Frisch, Hasslacher, Pomeau hexagonal lattice gas to study reaction-diffusion problems. Some numerical results are presented. We then consider the question of Galilean invariance from an "experimental" point of view, showing cases where the standard model is inadequate. Finally, we introduce a way to cure the Galilean disease and present some results of simulations for a few typical cases.

1. Introduction

The lattice gas technique first introduced by Pomeau et al. [1] and later refined by Frisch, Hasslacher, and Pomeau (FHP) [2] is now considered as an efficient way to simulate viscous flows at moderate Mach numbers in situations involving complex boundaries. However, it is unable to represent thermal or diffusional effects since all particles have the same speed and are of the same nature. In addition, the macroscopic behavior of the FHP (or standard) model is not Galilean invariant in the sense that the nonlinear advection term in the momentum equation involves an the original FHP model to study reaction-diffusion problems and then discuss the implications of $g(d) \neq 1$. Finally, we shall present a way to design a model that is Galilean invariant at least for low Mach numbers.

2. Extension of the FHP model

The original FHP model involves particles whose velocities $\mathbf{c}_i$ have the same modulus and point in the six possible directions corresponding to the links between one node of the lattice and its six nearest neighbors. It is useful to add rest particles (0 or 1 in the Boolean model) that are

involved in collisions of the type rest particle and n_i, with $i \in \{1,\ldots,6\}$, represents one of the six possible moving particles. Using the Rivet-Frisch method [3] to calculate the viscosity, or measuring it by relaxation of shear waves, it has been shown [4] that the maximum possible Reynolds number is obtained using the seven-bit model with all possible non-transparent collisions. With this criterion, the above model is thus preferred over the simpler models, and there are 76 non-transparent collisions among the 2^7 possible precollision states.

In a way similar to that of Burges and Zaleski [5], who introduced cellular automata adapted to the description of fluid mixtures, we start now from the original seven-bit FHP model and add seven other bits, one for each bit of the basic model, that may be interpreted as the type (or color) of the particle [6]. The state of the system is thus fully determined by giving at each node of the lattice $\{(n_i,t_i)\}$, $i \in \{0,\ldots,6\}$ where $t_i = 0$ for $n_i = 0$ and $t_i = 0$ or $t_i = 1$ for $n_i = 1$, ($t_i = 0$ particle of type A, $t_i = 1$ particle of type B). There are now 3^7 possible states.

The bit t_i is attached to and propagates as bit n_i. The collision rules can be of several types according to the type of problem being investigated.

This new model can be analyzed in the same way as the basic model. One may define as macroscopic quantities:

$\rho = \sum_i n_i$ total density
$\rho\mathbf{u} = \sum_i n_i \mathbf{c}_i$ total flux
$C = \frac{1}{\rho}\sum_i n_i t_i$ concentration of B particles.

At the macroscopic level, these quantities satisfy the continuity equation, the Navier-Stokes equation with a factor $g(d)$, and a concentration equation.

$$\partial_t \rho + div \rho \mathbf{u} = 0$$

$$\partial_t \rho u_\alpha + \partial_\beta(\rho g(d) u_\alpha u_\beta) = -\partial_\alpha P + \partial_\beta(\nu(\rho)\partial_\beta \rho u_\alpha)$$

$$\partial_t \rho C + \partial_\alpha \rho C u_\alpha = \partial_\alpha D(\rho)\partial_\alpha \rho C + \varpi(C)$$

where D is a diffusion coefficient and $\varpi(C)$ a source term when type exchange collisions are included.

Here, d is the average density of particles per cell, so that

$$g(d) = \frac{7(1-2d)}{12(1-d).}$$

2.1 Definition of collisions

The general rules that allow one to determine the output of any precollision situation are the following:

1. The total number of particles is conserved.

2. The total linear momentum is conserved.

Now the collisions can be nonreactive, which means that the numbers of A and B particles are conserved, or they can be reactive, which means that the numbers of A and B particles can vary.

Note that even for nonreactive collisions and distributions of velocities that correspond to no change in the $\{n_i\}$, the values of the $\{t_i\}$ can be redistributed when $\sum t_i$ differs from 0 or $\sum n_i$. In some cases, it is found that there are as many as 35 equivalent distributions of the $\{t_i\}$. This means that a poor model from the point of view of the viscosity (few efficient velocity redistributing collisions) may nevertheless lead to a small value of the diffusion coefficient.

The choice for the redistribution of the $\{t_i\}$ by reactive collisions is obviously huge. Here, we have first considered situations of the type:

$$A + A + B \underset{k_a^-}{\overset{k_a^+}{\rightleftharpoons}} A + A + A$$

$$A + B + B \underset{k_b^-}{\overset{k_b^+}{\rightleftharpoons}} B + B + B$$

where either A or B acts as some sort of catalyzer. In that case, the production rate is given by

$$\varpi(C) = k_a^+ C(1-C)^2 + k_b^- C^3 - k_a^-(1-C)^3 - k_b^+ C^2(1-C).$$

If we assume symmetry in the reaction rates, $k_a^+ = k_b^+ = k^+$ and $k_a^- = k_b^- = k^-$, then ϖ is an odd function of $C - 0.5$.

Let us define $\chi = k^-/k^+$. If $\chi < 1/3$, ϖ has three roots C_1, $C_2 = 1 - C_1$ and $1/2$. For $\chi = 0$, $C_1 = 0$ and $C_2 = 1$, which means that the system will exhibit segregation into regions which are filled with pure A or pure B.

This result can be extended to situations where all reactions

$$A + nB \underset{0}{\overset{k_n^+}{\rightleftharpoons}} (n+1)B$$

$$nA + B \underset{0}{\overset{k_n^+}{\rightleftharpoons}} (n+1)A$$

with $n > 1$ are included.

Note that this model implies no coupling between the type exchange and the dynamics of the particles and thus cannot represent such effects as surface tension.

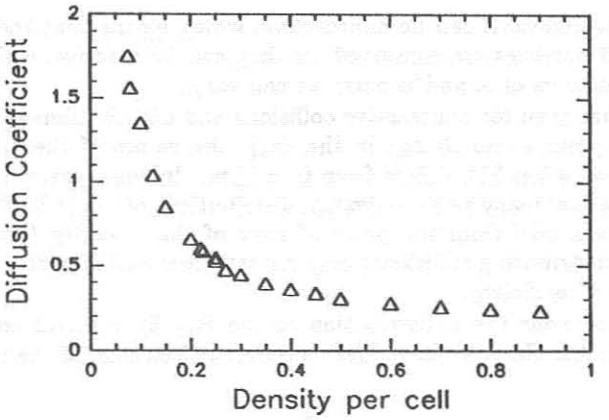

Figure 1: Measured value of the diffusion coefficient D versus density of moving particles per cell.

2.2 Experimental study

The dynamics of lattice gas mixtures has been studied by simulation on a FPS164 computer using the "table method", in which we use the state of each node of the lattice as an address in a collision table to determine the redistribution of the $\{(n_i, t_i)\}$. This method is not very efficient, as it implies reading the memory in a random manner, but it is very simple. The large indetermination in the outcome of some precollisional states (up to 35-fold in this model) is dealt with in the following manner: before each sweep through the lattice, we choose at random one particular outcome among tables containing the equivalent states.

2.2.1 Basic properties

We have determined the diffusion coefficient D by studying the time relaxation of either a concentration step or a sinusoidal modulation of the concentration. In the first case, a very good fit of the data with the standard solution of the diffusion equation is found. The resulting experimental determinations of D are shown in figure 1. Contrary to all results on the standard FHP model (which is dual in the sense that they depend only upon $\mid 0.5 - d \mid$) here D is smaller for $d > 0.5$. This comes from the fact that we have taken only $t_i = 0$ for $n_i = 0$. We could have decided to color the holes by taking $t_i = 1$ for $n_i = 1$ and $t_i = 0$ or $t_i = 1$ for $n_i = 0$. The model can be used to analyze how a tracer is dispersed by a flow [7].

We now allow type exchange reactions to take place. In that case, sharp interfaces are observed, the thicknesses of which are on the order of $\sqrt{D/k}$.

Detailed results are described in reference 6.

As mentioned previously, there is no surface tension for the present model when $k^+ = k^-$; thus, the interface between A and B exhibits a diffusive behavior. It can be shown that the dynamics of the interface is governed by $dx/dt = -D/R$ if x is a coordinate normal to the interface and R its radius of curvature. A sinusoidal interface will relax exponentially, and the radius of a circular bubble will decrease as $R^2(t) = R^2(0) - 2Dt$ [8].

The model will be adequate to study hydrodynamics with free boundaries, provided that the relevant time scales are short compared to that of the diffusion of the interfaces. It is therefore preferable to use a density of 0.75 rather than 0.25; the hydrodynamics is the same, but D is smaller.

This model, to which gravity can be added, provides a simple way to study phenomena such as the Rayleigh-Taylor instability [9]. Here we will illustrate its possibilities with some results for the Kelvin-Helmholtz instability.

2.2.2 Kelvin-Helmholtz instability

Two parallel plates of length 1024, separated by 256 lattice sites, are set as boundaries for a channel assumed to be periodic in the direction of the plates. Stick conditions are implemented by imposing velocity reversal of particles colliding with the boundary. The initial conditions for the experiment are

1. half of the channel is filled with particles of type A and velocity $+v$ parallel to the plates, and
2. the other half is filled with B particles and velocity $-v$.

The mean density of moving particles is 0.75 and $v = 0.21$. Maps of the local average of the particle fluxes are computed for various values of time. Note that color-blind maps are identical to those which would be obtained with the standard FHP model with the same microscopic initial distribution of the $\{n_i\}$.

In a first experiment, the collision rules include only nonreactive diffusion of A and B particles. Figure 2 shows isoconcentration curves for A at time $t = 3000$. For this particular run, in one portion of the channel, the interface was destabilized by the Kelvin-Helmholtz instability and A particles were advected by the flow, whereas in another portion of the channel, the interface remained stable and uniform diffusion took place. (This particular result is not typical; usually, the $k = 4$ mode is the most unstable.)

In a second experiment, we use the autocatalytic reactive rules. Figure 3 shows the distribution of the flux of B at time $t = 2000$, and figure 4 shows several successive shapes of the interface that remains sharp for several thousand time steps.

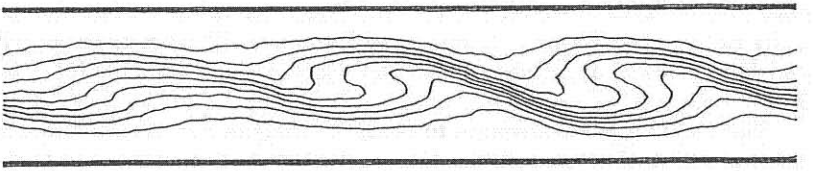

Figure 2: Isoconcentration curves (for $C = 0.10to.90$) in the situation leading to the Kelvin-Helmholtz instability at time $t = 3000$. Purely diffusive case.

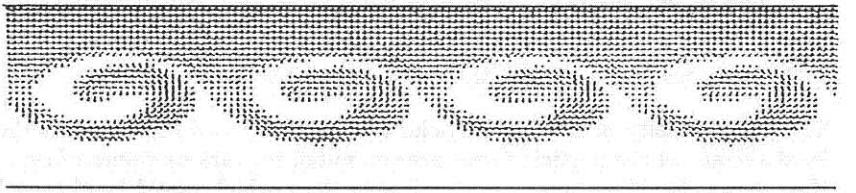

Figure 3: Map of B particle flux at time $t = 2000$ in the situation leading to the Kelvin-Helmholtz instability, using type exchange reactions that allow phase separation.

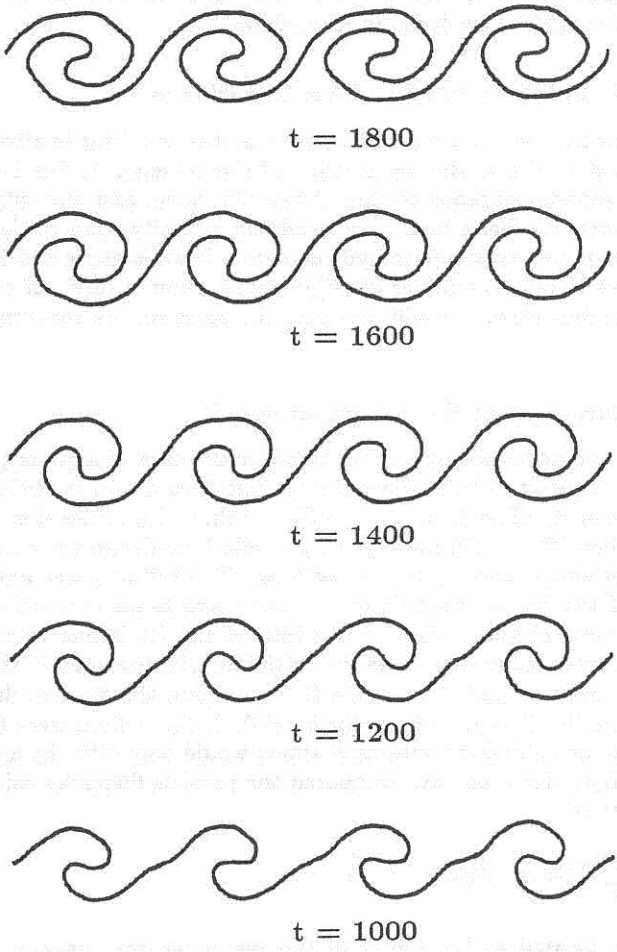

Figure 4: Series of shapes of the interface separating phase A and phase B in the situation leading to the Kelvin-Helmholtz

The results shown here need to be supplemented by quantitative tests. The fact that the advection terms of the total momentum and concentration are different should be analyzed in more detail.

3. Experimental study of Galilean invariance

The equation for the total momentum shows that vorticity is advected at speed $g(d)u \neq u$, if u is the mean value of the velocity. It has been proposed that nonhomogeneous scaling of velocity, time, and viscosity would allow "restored" Galilean invariance, and the quantity used to define the ability of the model to simulate hydrodynamic flows is expressed in terms of an effective Reynolds number $ulg(d)/\nu$ rather than in terms of the usual Reynolds number ul/ν. We will now describe some results concerning this question.

3.1 Measurement of the advection speed

To measure the advection speed, we consider the case of a jet of particles A in a bath of particles B. The densities of particles A and B are identical. The initial velocity of particles A is $v+U_0$ and that of particles B is $-v+U_0$. The lattice has 1024×256 nodes, and periodic boundaries are assumed in both the horizontal and vertical directions. The initial lower and upper interfaces of the jet are modulated so that there is no random effect in the development of the eddies. The width of the jet is one third of the height of the system, so that when flat initial interfaces are used, the $k = 3$ mode is the most unstable one. We then compare the time evolution of two flows, one for $U_0 = 0$ and one for $U_0 \neq 0$. If the system were Galilean invariant, the two flux distributions at time t would only differ by a uniform translation $U_0 t$. Here, we have compared the particle fluxes by calculating the minimum of

$$Z = \sum_{lm} \{\mathbf{j}(\mathbf{r}_{lm}) - \mathbf{j}(\mathbf{r}_{lm} + \mathbf{x})\}^2,$$

where $\mathbf{r}_{lm}$ is located at the center of the averaging box (usually 16×16 sites are used). We show in figure 5 the value of x_{min} corresponding to the minimum of Z. The data on the top correspond to $U_0 = 0.215$; the other correspond to $U_0 = 0.128$. The mean density per cell is 0.30. The crosses are experimental; the solid lines are given by $g(d)U_0 t$. This provides a good verification of the non-Galilean nature of the system, as the eddies are found to be advected at speed $g(d)U_0$. Similar results apply up to approximately $U_0 \simeq 0.25$, meaning that the higher order terms in the momentum equation can be neglected in the present situation for Mach numbers up to roughly 0.4.

We also find that the minimum value of Z, the error, remains approximately equal to that obtained when comparing two different microscopic realizations of the same macroscopic conditions.

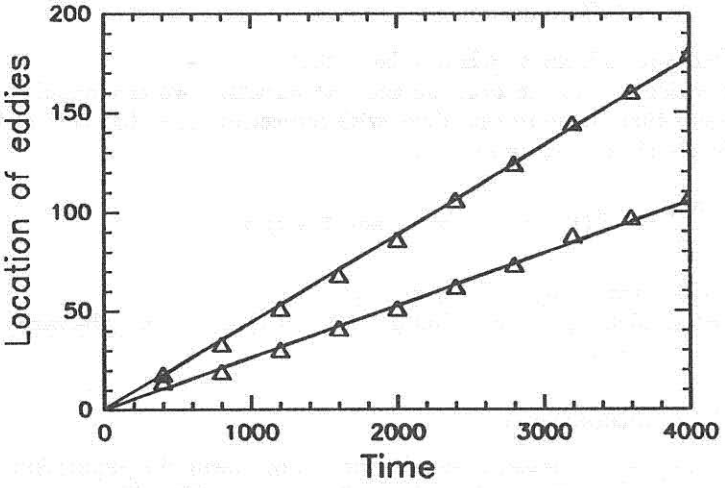

Figure 5: Value of the displacement between two flows. Crosses are determined experimentally; solid curves correspond to the advection speed $U_0 g(d)$.

Another way to study non-Galilean invariant problems would have been to analyze how small eddies are advected by large ones. Significant results would be obtained only for lattices much larger than the one used here in order to avoid viscous relaxation of the small eddies [10].

We have also considered the Kelvin-Helmholtz situation with reactive collisions and found dramatic differences between the results obtained for $U_0 = 0$ and $U_0 \neq 0$. In particular, we find that the roll-up of the interface does not take place when $U_0 \neq 0$.

3.2 New lattice gas with $g(d) = 1$

The absence of Galilean invariance of the original model is due to the use of a finite set of directions for the velocity and to the exclusion principle that leads to the Boolean character of the particles. In general, g is given by

$$g(d) = \frac{D \sum_i d_i \ \sum_i d_i(1-d_i)(1-2d_i)c_i^4}{(D+2)\{\sum_i d_i(1-d_i)c_i^2\}^2}$$

if d_i is the density of particles per cell and D the dimensionality. At equilibrium for $u = 0$, the total density is given by $\rho = 6d + d_0$ if d_0 is the density of rest particles. The standard seven-bit model leads to $d_0 = d$ so that

$$g(d) = \frac{7(1-2d)}{12(1-d)}.$$

One way to increase g is to take $d_0 > d$.

Keeping one bit to describe the rest particles, we can unbalance the collisions that create rest particles with respect to those that destroy them. In the simplest case, we can take

$$\frac{dn_0}{dt} = 6d^2(1-d)^4(1-n_0) - 6xd(1-d)^5 n_0$$

so at equilibrium, $n_0 = d/(d+x-dx)$.

For small d, $n_0 = d/x$ so that $g = (1+1/6x)/2$, that may be taken equal to 1 for $x = 1/6$.

3.2.1 Collision rules

Here, we propose to use a two-bit word to represent the population of the center (n_0, m_0), with the following collision rules. All collisions conserving total number and total linear momentum are included [11]. The collisions leading to creation and destruction of rest particles are all included, except a few cases which take place with probability x, y, or z. For details, see table 1, where all collisions considered here are indicated for one of the six possible directions of the velocity vector.

It may be shown that the equilibrium value of n_0 and m_0 are solutions of the following coupled equations:

$$\{(1-d)^4d^2+2(1-d)^3d^3+(1-d)^2d^4+(1-d)d^5\}(1-m_0) = x(1-d)^5d(1-m_0)n_0$$

$$+ z\{(1-d)^5d + (1-d)^4d^2 + 2(1-d)^3d^3 + (1-d)^2d^4\}m_0n_0$$

$$\{(1-d)^4d^2+2(1-d)^3d^3+(1-d)^2d^4+(1-d)d^5\}m_0(1-n_0) = y(1-d)^5d(1-m_0)n_0$$

Analyzing the numerical values of n_0, m_0, and the corresponding $g(d)$, it is found that for $x = 0.5, y = z = 0.20$, there exists a value of d for which $g(d) = 1$ and $dg(d)/dd = 0$.

For simplicity of the dynamics, we prefer to use the case $x = 1/2, y = z = 1/6$, which leads to a theoretical value of $g_{max} = 1.072$ for $d = 0.17$ and $g = 1.0$ for $d = 0.21$.

The model can now be analyzed with the Chapman-Enskog method, as was done by Rivet and Frisch for the standard model. This allows us to determine the kinematic shear viscosity

$$\nu = \frac{1}{4(C_{11} - C_{12} - C_{13} + C_{14})} - \frac{1}{8}$$

with

input		output		probability
moving particles	rest particles	moving particles	rest particles	
	1 2 3		0 1 2	x y z
	0, 1 or 2 3	 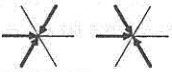	1, 2 or 3 2	1 z/2 z/2
	0, 1, 2 or 3	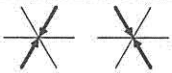	0, 1, 2 or 3	1/2 1/2
	0, 1, 2 or 3		0, 1, 2 or 3	1
	0, 1 or 2 3	 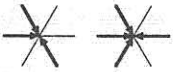	1, 2 or 3 3 2	1 1-z z
	0, 1 or 2 3	 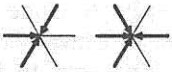	1, 2 or 3 3 2	1 1-z z
	0, 1 or 2 3	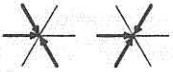 	1, 2 or 3 2	1/2 1/2 z
	0, 1, 2 or 3	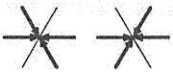	0, 1, 2 or 3	1/2 1/2
	0, 1 or 2		1, 2 or 3	1

Table 1: Details of the collisions considered in the Galilean invariant lattice gas model.

$$C_{11} - C_{12} - C_{13} + C_{14} =$$
$$5A_{41} + 11A_{32} + 10A_{23} + 6A_{14} + 2A_{05}$$
$$+ m_0 n_0(-2A_{41} + 4A_{32} + 5A_{23} - 3A_{14} - 2A_{05})$$
$$+ 2(A_{50} + A_{41})(xm_0(1 - n_0) + y(1 - m_0)n_0)$$
$$+ zm_0 n_0(2A_{50} + 3A_{41} - 5A_{32} - 4A_{23} + 2A_{14})$$

where $A_{ij} = (1-d)^i d^j$

We plot in figure 6 the theoretical values of $g(d)$, $g(d)/\nu$, and η which appear in the Reynolds number and characterize the ability of the model to represent flows. It is interesting to note that we have improved the value of the Reynolds number.

3.2.2 Numerical results

The new eight-bit lattice gas has been implemented on a computer. The equilibrium value of $\rho(d)$ is in fair agreement with the theoretical value deduced from the equations for n_0 and m_0.

We have also measured the advection speed. Instead of using the same situation used previously, we have studied the relaxation of a moving shear wave. For this purpose, we consider a 512×512 lattice with periodic boundary conditions and impose as initial conditions

$$v(\mathbf{r}, 0) = v_x + v_y \cos \mathbf{k}.\mathbf{r} \quad \text{with } \mathbf{k} \parallel \mathrm{Ox}.$$

We determine the spatial phase ϕ of the k-Fourier component of $v_y(t)$. It is found to vary linearly with time, and we plot $\mathrm{d}\phi/\mathrm{dt}$ in figure 7 together with its theoretical value $g(d)v_x k$. Good agreement is obtained, showing that the model is truly Galilean invariant for a particular but adjustable density (here, $d = 0.21$). Moreover, to first order, the invariance is not destroyed by small density fluctuations.

Preliminary measurements of the speed of sound and of the kinematic shear viscosity are in good agreement with the theory.

The new model should be very useful but requires further investigation, especially with regards to the fact that some collision events do not satisfy semi-detailed balance. Adding color to the new model involves no particular difficulty.

4. Conclusion

In this paper, we have presented two extensions of the basic FHP lattice gas model. The first one adds a second bit to each of the seven-bit occupation numbers. It allows the simulation of various diffusion-reaction problems and of hydrodynamic flows with free boundaries. The second allows achievement of true Galilean invariance for a limited range of the density, at the cost of using an extra bit for the rest particles and the lack of semi-detailed balance for a subset of the collisions.

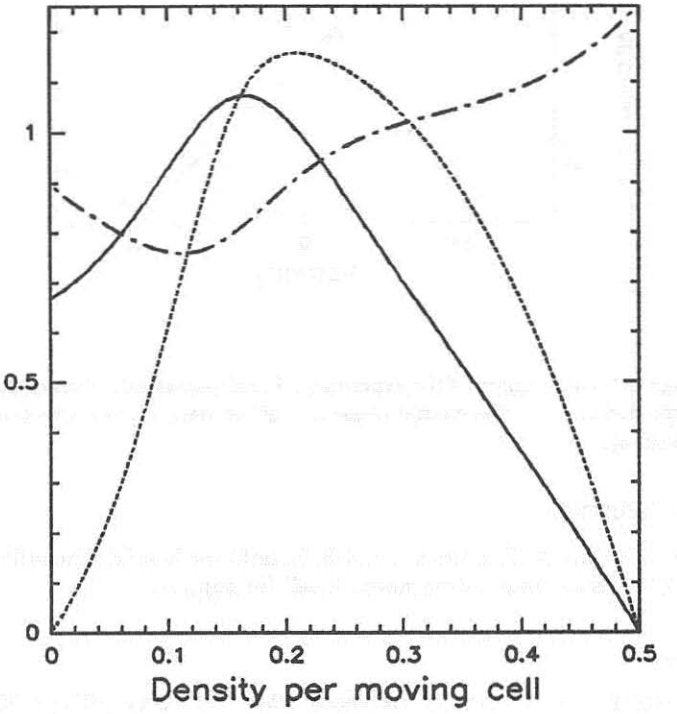

Figure 6: Theoretical values of $g(d)$ (solid line), $0.2 \times g(d)/\nu$ (dotted line), and $25 \times \eta$ (dash-dot line) versus density of moving particles per cell for the new model, when $x = 1/2$ and $y = z = 1/6$.

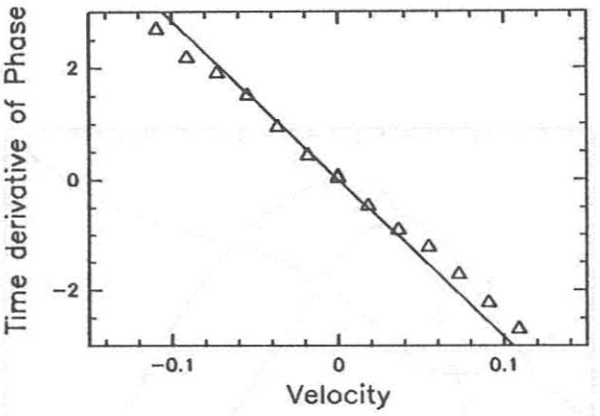

Figure 7: Comparison of the experimental and theoretical values of the time derivative of the spatial phase of a shear wave versus advection speed v_x.

Acknowledgments

We thank P. Clavin, Y. Pomeau, and S. Zaleski for helpful discussions and GRECO 70 "Expérimentation numérique" for support.

References

[1] J. Hardy, O. de Pazzis and Y.Pomeau, *Phys. Rev.*, **A13** (1976) 1949.

[2] U. Frisch, B. Hasslacher and Y. Pomeau, *Phys. Rev. Letters*, **56** (1986) 1505.

[3] J. P. Rivet and U. Frisch, *Compt. Rend. Acad. Sci. Paris*, **II 302** (1986) 267.

[4] D. d'Humières and P. Lallemand, *Physica*, **140A** (1986) 327.

[5] C. Burges and S. Zaleski, *Complex Systems*, **1** (1987) 31.

[6] P. Clavin, P. Lallemand, Y. Pomeau, and G. Searby, *J. Fluid Mech.*, to be published.

[7] J. P. Hulin and C. Baudet, to be published.

[8] D. d'Humières, P. Lallemand and G. Searby, *Proc. of E.P.S. Int. Conf. on Physico-chemical Hydrodynamics* (La Rabida, Spain, July 1986), M. G. Velarde, ed. (Plenum Press 1987).

[9] D. d'Humières, P. Clavin, P. Lallemand, and Y. Pomeau, *Comp. Rend. Acad. Sci. Paris*, II **303** (1986) 1169.

[10] S. Wolfram, private communication.

[11] D. d'Humières and P. Lallemand, "Numerical Simulations of Hydrodynamics with Lattice Gas Automata in Two Dimensions", *Complex Systems*, **1** (1987) 598.